Glass Europe Vol. 2 (2024) 45-54
https://doi.org/10.52825/glass-europe.v2i.1320

Submitted: 03 May 2024 | Accepted: 02 Aug. 2024 | Published: 09 Aug. 2024

Open Electrode Thermal Poling Setup for Treating Lithium-Aluminosilicate Glass-Ceramics Using Gas Discharge

Jonas Hildebrand and Christian Roos

Institute of Mineral Engineering, RWTH Aachen University, Aachen, Germany

*Correspondence: Jonas Hildebrand, jonas.hildebrand@rwth-aachen.de

Abstract. A setup for thermal poling treatment of glass and glass-ceramic via gas discharge using an open electrode configuration was built and tested successfully. In the setup a thin Pt-wire is used as a top electrode with adjustable distance to the glass sample. The glass rests on a Pt-sheet acting as bottom electrode which again rests on transporting rolls made of alumina. The setup is implemented in a specially built furnace in which the sample is moved underneath the static wire electrode. With this setup, lithium-aluminosilicate (LAS) glass samples were thermally poled at 200 °C for 20 min, 60 min and 180 min with discharge currents ranging from 25 µA to 300 µA. Over time the process gets more unstable but without any major breakdowns. The measured crystallinity at the anode side surface of the post-poling ceramised samples shows a decrease with both treatment time and poling current (i.e. electrical field strength). This is explained with the depletion of Li from the anode side surface layer which becomes stronger with higher electrical fields and continues over time. In scanning electron microscopy (SEM) images of cross sections of the anode sides a mostly glassy layer is observed which adds to the point aforementioned. As a key result this work proved that with an open electrode setup for thermal poling treatments of LAS glasses similar results can be achieved as with a blocking setup. This opens the door to the modification of glasses and corresponding glass-ceramics in an inline and continuous process that can be used industrially.

Keywords: Glass-Ceramics, Thermal Poling, Gas Discharge

1. Introduction

A first model for the phenomenon of “electrode polarization” was established by Carlson et al. in 1972 [1]. It was found that by applying a direct current (DC) potential across a glass sample at elevated temperatures a thin surface region facing the anode is altered in chemistry and structure. The formation of a high electric field in this area causes mobile cations that are present in the glass network to drift away from the anode towards the cathode. With this the so-called depletion layer is formed in which negatively charged nonbridging oxygens (NBOs) are left [2]. According to the single charge motion model by Von Hippel [3], the thickness of this layer should be in the range of tens of nanometres. In contrast, the depletion layer thicknesses measured in several studies are in the range of micrometres [2], which leads to the conclusion that negative charges need to be compensated for the depletion layer to grow further. One compensation possibility is the recombination of nonbridging oxygens which leads to structural changes of the glass network towards a more silica like structure with higher degree of polymerisation [2], [4] which in turn leads to property changes of the depletion layer [4], [5].

The thermal poling treatment is often done by placing a plane glass sample between two electrode plates which are used as anode and cathode [1], [2], [6], [7], [8], [9]. The electrodes can be blocking or non-blocking regarding the surrounding atmosphere which influences the poling process [2]. For a blocking anode the possible negative charge compensation methods discussed in literature are oxygen drift and electron drift towards the anode. Both will lead to the formation of molecular O_2 due to the aforementioned recombination of excess NBOs [8]. When a non-blocking anode is used, particles from the atmosphere (e.g. H_3O^+) can enter the glass surface and compensate negative charges [2].

For an open electrode setup different possibilities exist which differ in the form of the electric field. When electrode plates with a certain roughness are used, small gaps between the electrodes and the glass surface allow the surrounding atmosphere to enter the thermal poling process while keeping direct contact between the electrodes and the glass [2], [5], [9]. On the other hand, gas discharge or corona discharge treatments can be used when separating at least one electrode completely from the glass surface. Often, an inhomogeneous electric field is used for the discharge process by utilising a needle to plane electrode configuration [10], [11], [12], [13]. The electric field is concentrated at the needle tip (in general at small radii of the electrode surface) leading to field strengths above the breakdown voltage of the atmosphere in a small volume around the tip. This leads to the generation of ions which will move along the electric field lines towards the glass surface and eventually build up the electric field across the glass sample [10]. Alternatively, the electrodes can be a wire to wire or wire to plane configuration to create a homogeneous electric field along the wire length. In combination with a moving sample perpendicular to the wire, it is possible to apply the electric field to the whole sample surface over time to achieve a thermal poling treatment [14].

The focus in thermal poling research with glasses was on the effects on soda-lime-silicate glasses. Sander et al. [15], [16] transferred the method to glass-ceramics by performing thermal poling with blocking electrodes on lithium-aluminosilicate (LAS) glasses. In these experiments a 500 nm thin, mostly amorphous layer remained on the anode side surface after the crystallisation of the treated glass samples. X-ray diffraction (XRD) and scanning electron microscopy (SEM) measurements revealed a rising crystal content with increasing information depth in an approximately 15 µm thin surface layer as well as different crystal grain sizes in the layer and the bulk material. It is believed that the Li-depleted surface layer after the treatment impedes the crystallisation and therefore leads to a smaller crystallinity in the depletion layer, as Li is one of the main components of the formed high quartz solid solution (HQSS) in these glass ceramics.

It has been shown that thermal poling alters the chemical durability [17], [18], [19], [20], strength and hardness [5], [21], and also optical properties of soda-lime-silicate glass surfaces [22], [23], [24], [25], [26]. In this work a setup similar to [14] was developed and tested for the thermal poling treatment of LAS glasses and glass-ceramics with the long-term aim to transfer the benefits of thermal poling on SLS glasses to glass-ceramic systems. The influence of the poling time and discharge current on the crystallinity of the final glass-ceramics was evaluated using XRD and SEM and compared to the work of Sander et al.

2. Experimental

The developed thermal poling setup uses a wire to plane electrode configuration consisting of a platinum sheet (100 x 100 mm^2) as bottom electrode and a platinum wire (diameter 0.35 mm) as top electrode. The wire is stretched between two high-temperature-resistant steel prongs to straighten it and is placed parallel to the sample surface. The steel holder leads through a hole in the furnace ceiling out of the furnace where it is mounted to a vertically adjustable platform. With that the distance between the wire electrode and the sample surface can be set precisely to any chosen value. The platinum sheet electrode rests on a glass-ceramic plate which is placed on alumina rolls in a special furnace built by Thermo-Star GmbH. These rolls

can be programmed to turn in both directions and therefore move the bottom electrode with the glass sample back and forth underneath the wire electrode. The glass sample is placed on top of a graphite spacer slightly smaller than the sample surface area to prevent direct arcing between the two electrodes.

The Atmosphere around the sample can be controlled by injecting different gases through a 3D printed ceramic gas nozzle, directly above the wire electrode. A detailed sketch of the setup is shown in Figure 1.

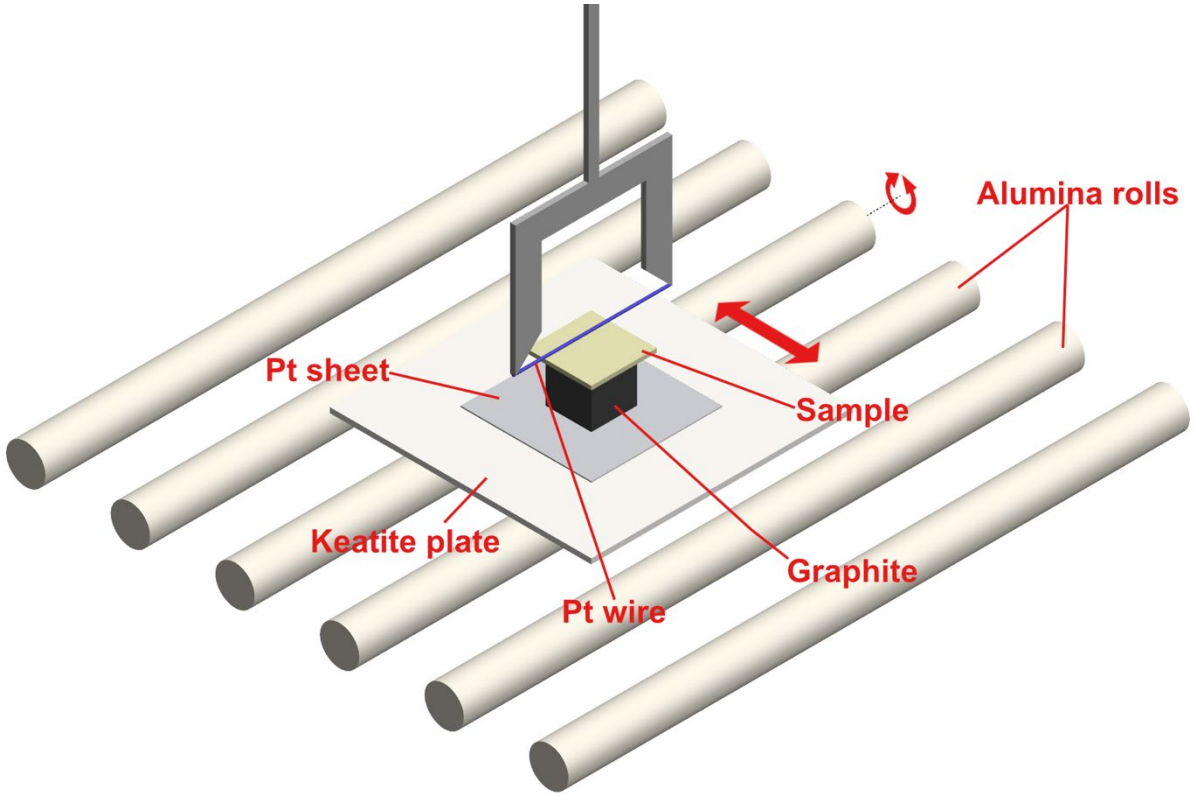

Figure 1. *Sketch of the new setup*

The described setup allows the investigation of the effect of different process parameters on the properties of thermally poled glasses and glass-ceramics. Varied parameters are sample size, treating temperature, electric field strengths and poling atmosphere, especially water containing ones.

To test the experimental setup, LAS glasses provided by Schott AG (composition is given in Table 1) were poled at 200 °C with discharge currents from 25 µA to 300 µA and poling times from 20 to 180 minutes. A detailed overview of the varied parameters is given in Table 2. The glass samples were cut from 200 mm x 200 mm glass sheets to sizes of 25 mm x 25 mm. To ensure a consistent surface quality, all samples were ground and polished in six steps ending with 1 µm diamond polishing suspension. Afterwards all samples were etched for 3 minutes in a 1:1 mixture of H_2SO_4 and HF to eliminate any remaining polishing traces.

Table 1. *Composition of the used LAS glass.*

Oxide	Mass fraction in %	Oxide	Mass fraction in %
SiO_2	66.73	ZrO_2	1.20
Al_2O_3	19.22	As_2O_3	0.99
Li_2O	3.77	BaO	0.84
TiO_2	2.72	HfO_2	0.32
MgO	2.05	K_2O	0.26
ZnO	1.85	Na_2O	0.13

The high voltage was applied using an “SHR” high voltage source from “iseg Spezialelektronik GmbH” with an integrated measuring unit to monitor the effective voltage and current. After each thermal poling treatment, the sample was removed from the furnace at 200 °C to quickly cool to room temperature and freeze-in the effects of the treatment. All samples were stored in a desiccator and ceramised simultaneously by heating to 860 °C with 10 $K \cdot min^{-1}$, dwelling 10 minutes und letting the furnace cool down afterwards. The achieved glass-ceramics were analysed using XRD with grazing incidence angles and SEM imaging. The XRD measurements were performed on an Empyrean 3rd Gen. from Malvern PANalytical using a chromium x-ray tube with $\lambda_{Cr,K\alpha}$ = 2.28976 Å, U = 30 kV and I = 55 mA. Measurements of the anode side surfaces were made under 10 different incident angles ranging from 0.4° to 20° to increase the information depth with each step. The obtained diffractograms (see Figure 2 as an example) were analysed using the Rietveld refinement technique and an external SiO_2-standard was used to calculate the mass fraction of high quartz solid solution with the K-factor method [27].

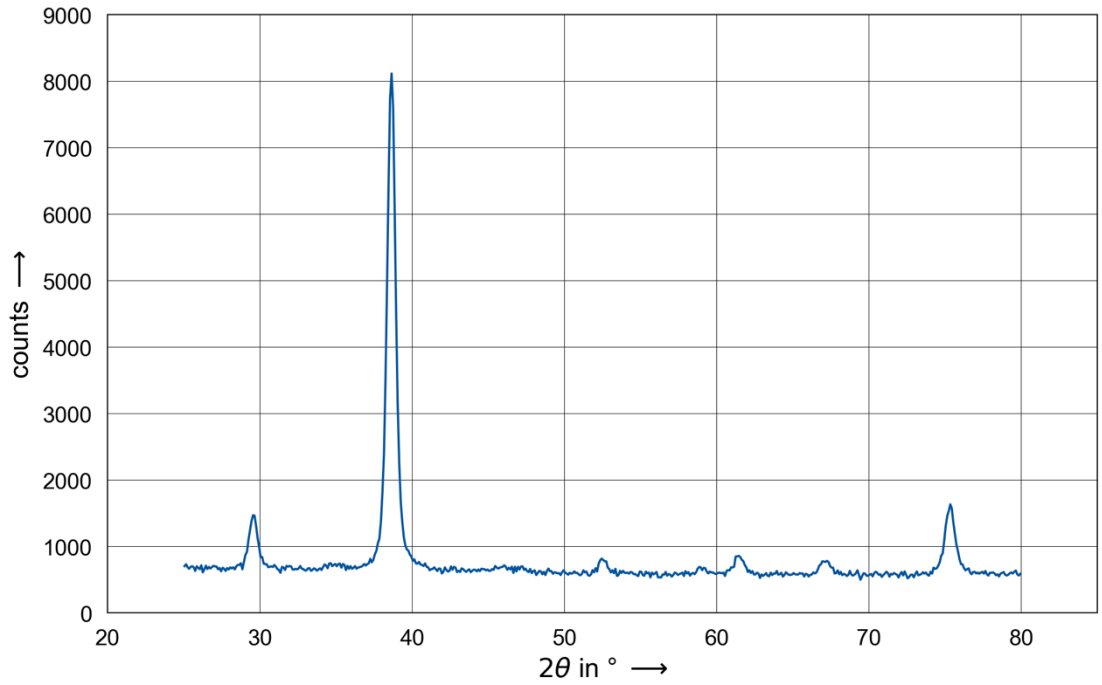

Figure 2. *Diffractogram of sample GC02-16 at an incidence angle of ω = 10°. All Peaks can be assigned to a high quartz solid solution phase.*

SEM imaging was performed on a Zeiss GeminiSEM with 1 keV acceleration voltage using secondary electron detection mode after polishing the cross section of the samples in 4 polishing steps up to 0.6 µm diamond suspension and etching the samples in a 1:1 mixture of 10 % H_2SO_4 and 2 % HF (volume fractions) to achieve a visible difference between the glass and the crystal phase in the SEM images.

Table 2. *Poling parameters and associated sample numbers.*

poling current / poling time	25 µA	50 µA	100 µA	200 µA	300 µA
20 min	GC02-01	GC02-02	GC02-03	GC02-04	GC02-05
60 min	GC02-06	GC02-07	GC02-08	GC02-09	GC02-10
180 min	GC02-11	GC02-12	GC02-13	GC02-14	GC02-15

3. Results and Discussion

During each thermal poling treatment both the current and voltage were monitored. Figure 3 shows a plot of both measured values over treatment time for sample GC02-15. The voltage as well as the current show a box profile (see smaller inset in Figure 3) where the maximum voltage of 4000 V is reached during the minimum current of 0 µA and vice versa. The maximum values correspond to the set maxima of 4000 V and 300 µA whereas the current vanishes completely, and the voltage decreases to around 3200 V. This characteristic profile origins from the movement of the sample beneath the top wire electrode. The rolling distance of the alumina rolls was set to 40 mm, so with a buffer distance of 7.5 mm to each side of the samples to compensate for small deviations in the sample positioning and to therefore ensure a poling treatment of the whole surface area. When the sample is exactly under the wire, and with that the distance between the wire electrode and the sample surface is equal to the set distance of 2 mm, the electric field gets strong enough to lead to a gas discharge and the maximum current flows at a voltage required for this but lower than the set maximum. As the sample moves horizontally, at one point it is in the buffer region of the rolling distance and not right under the top electrode anymore. Now the voltage rises to the maximum value to counterbalance the increasing distance between the top electrode and the sample surface. When the horizontal distance in addition to the vertical distance of 2 mm becomes too large, the electric field is not strong enough to maintain the gas discharge so that the current decreases to 0 µA. As the sample moves back and forth periodically the increase and decrease of voltage and current also follows a periodic pattern.

For longer poling times the current becomes more unstable as can be seen in Figure 3. The voltage increases slowly with poling time to counteract the decrease of the electrical conductivity of the glass due to the ongoing Li depletion from the anode side surface and to maintain the set maximum current. This effect leads to a constantly growing electric field strength. Simultaneously, the setup can be seen as a wire-plate capacitor and as the dielectric constant ϵ_r of the glass between the electrodes decreases, the capacitance C increases, see equation 1.

$$\boldsymbol{C = \frac{2\pi\epsilon_0\epsilon_r l}{\cosh^{-1}\left(\frac{d}{R}\right)}} \tag{1}$$

in which ϵ_0 is the vacuum permittivity, l and r are the length and the radius of the wire, d is the distance between the wire and the plate electrode. The energy of a capacitor is stored in its

electric field and thus the electric field strength rises with increasing capacitance. In combination with the rising voltage, this leads to an increasing possibility of electrical breakdowns and therefore to a more unstable process over time.

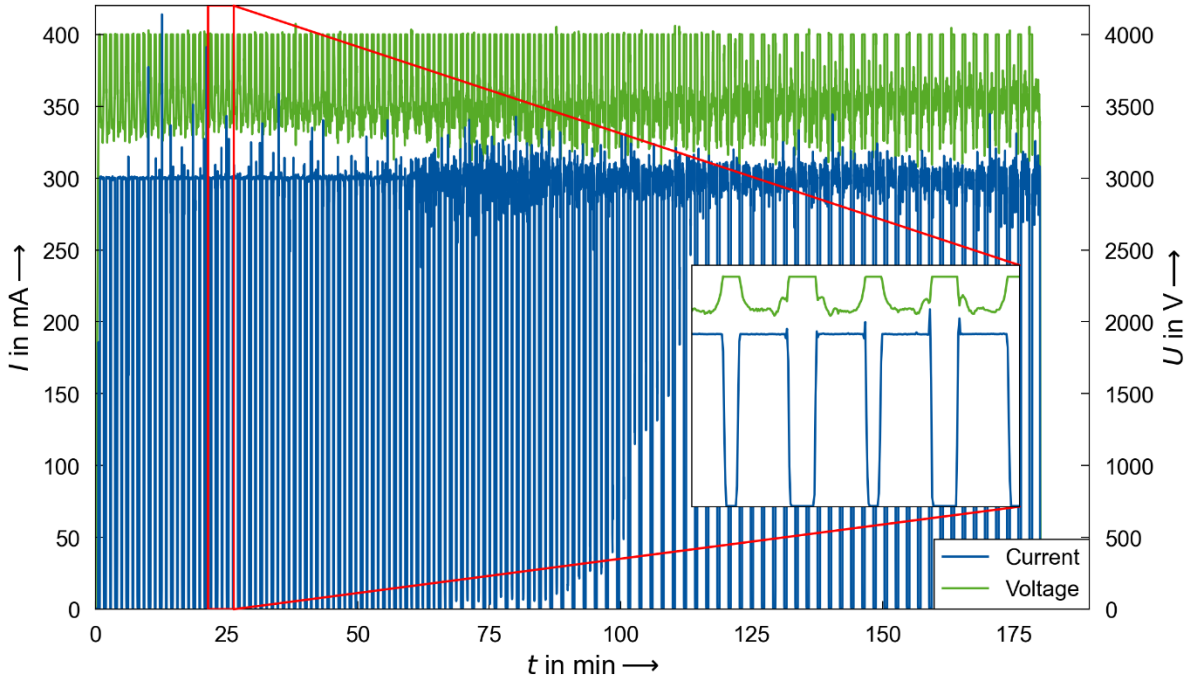

Figure 3. *Current and Voltage during poling treatment of sample GC02-15 for three hours at 200 µA. The characteristic box profile of both measured values is visible in the smaller inset.*

The progression of the crystal phase fractions over depth from the anode side surface plotted in Figure 4 show that both a higher poling current, which is accompanied by a higher poling voltage and therefore a stronger electric field, and a longer treatment time lead to less crystallinity in the surface layer. This is in good agreement with Sander's findings for a blocking anode setup [16] and can be explained with the depletion of Li, as done before. For the 180 minutes poled samples (Figure 4 c), the curve progressions of the reference sample and the samples poled with more than 100 µA show a different overall shape. The crystallinity of the reference sample increases from about 40 % to 70 % in the first two micrometres and grows slowly to values over 80 % for greater depths. In contrast, the poled samples show a decrease of the crystal content from about 10 % to values smaller than 5 % in the same two micrometres. From there the crystallinity grows steadily to bulk values. This effect can be explained by two phenomena. Firstly, the higher crystal content right at the surface compared to 2 µm depth in the poled samples could be caused by surface crystallisation or atmosphere interaction during the ceramisation. Secondly, also during ceramisation, a back diffusion of Li into the depletion layer can reduce the effect of thermal poling and lead to a smooth transition of crystallinity to bulk values as in the reference sample. Again, this curve progression is similar to Sander's results [16].

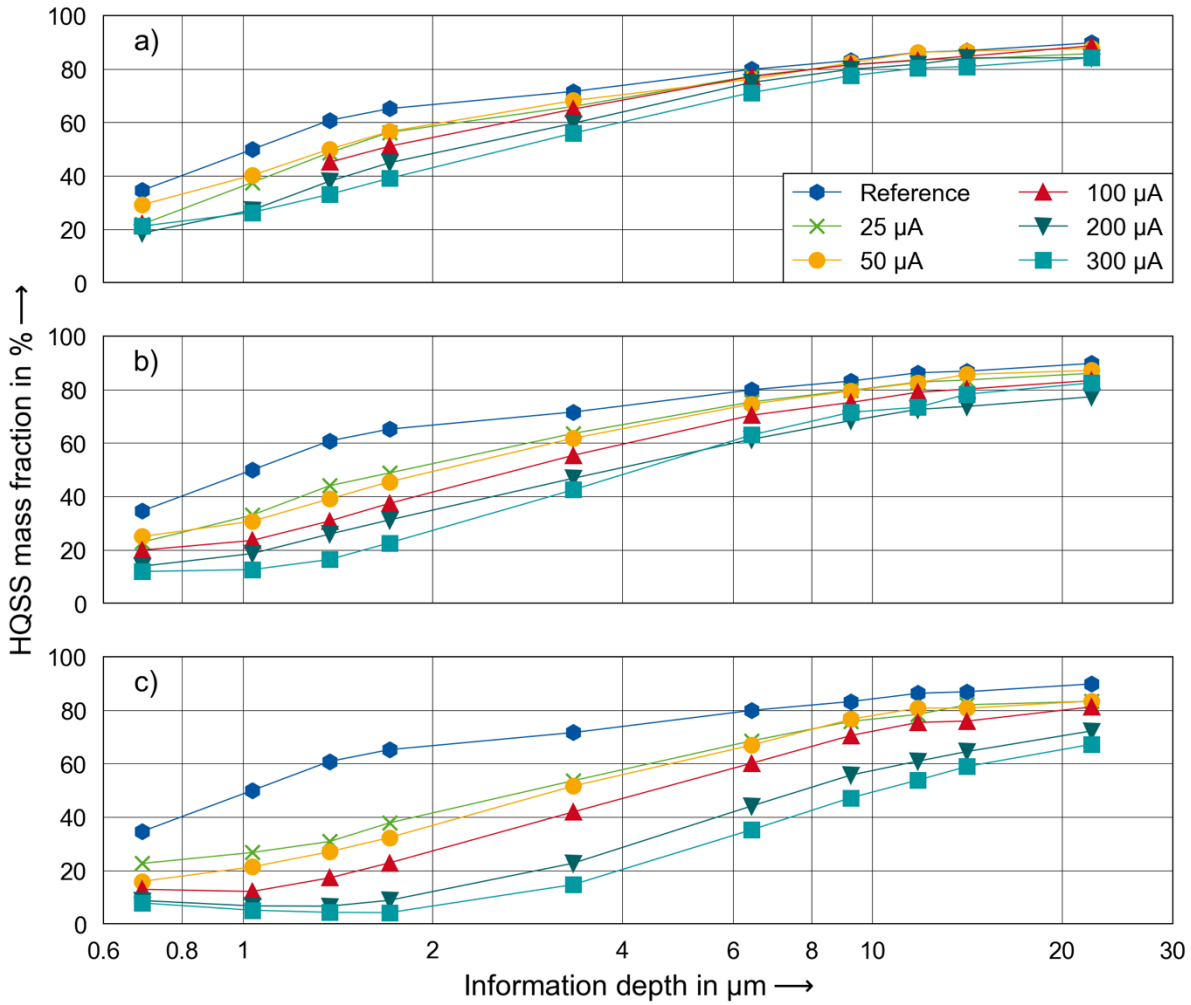

Figure 4. *Development of the mass fraction of the high quartz solid solution with depth from the anode side surface of samples poled for a) 20 minutes, b) 60 minutes and c) 180 minutes. Note: No error bars were included into this plot as from the mathematical operation during Rietveld refinement no error arises. There should be a measurement uncertainty due to instrumental fluctuations and the operator, but this should be in the range of 1-2 %. Additionally, as it was always the same person doing the measurements and refinements the occurring uncertainty should be systematic and therefore not influence the comparison between the samples.*

In the SEM images of the cross sections of samples GC02-03, 08 and 13 a several hundred nanometre thin mostly glassy layer can be observed at the anode side surface, see Figure 5. The thickness of this layer grows and the visible crystallinity decreases with treatment time. For the 20 minutes poled sample it is ~200 nm thin, for the 60 minutes poled sample ~300 nm and for the 180 minutes poled sample it extends to ~400 nm. This behaviour indicates that with treatment time and therefore growing depletion layer and structural rearrangements in the depletion layer this glassy surface layer grows in thickness. Overall, the SEM images are in good accordance with the XRD results, as a longer treatment time leads to less crystallinity in the analysed surface layer.

Regarding the transparency of the thermally poled glasses before and after ceramisation, no differences between the samples and in comparison to the untreated reference sample GC02-16 could be seen. All samples showed the same weak yellow tint before crystallisation and a stronger yellow tint afterwards.

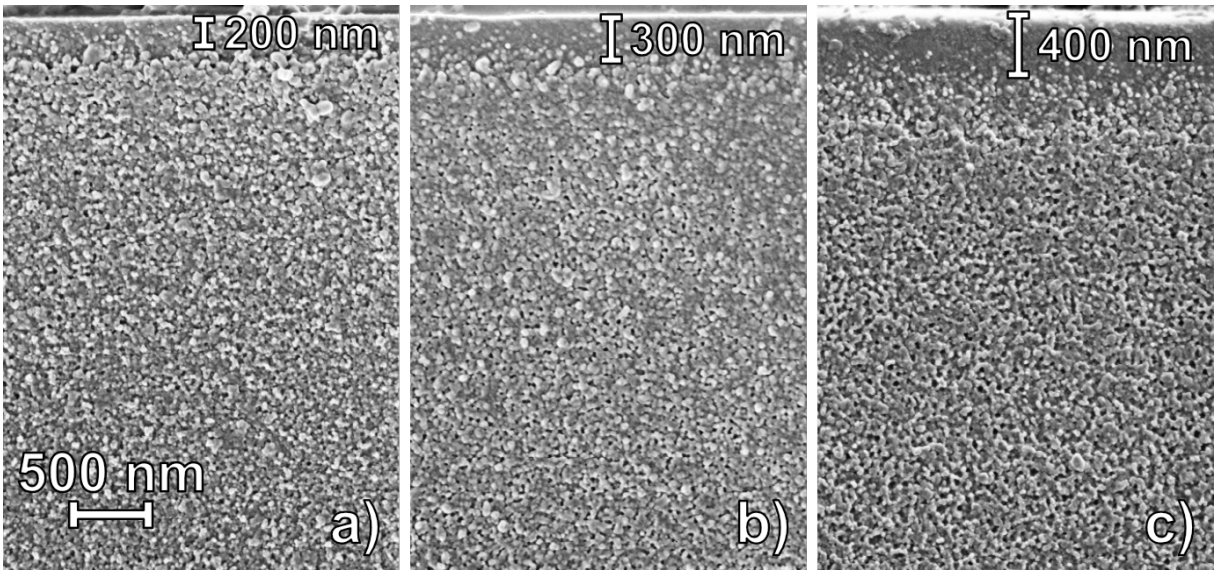

Figure 5. *SEM images of cross sections of the anode sides of 100 µA poled samples GC02-03 (20 min), GC02-08 (60 min) and GC02-13 (180 min).*

4. Conclusion

A setup for thermal poling treatments of glasses and glass-ceramics using an open electrode configuration (similar to [14]) was built and tested successfully on LAS glasses. The results of a first sample series show the formation of a depletion layer and its influences on the final glass-ceramics in very good accordance with the results of Sander et al. Both XRD and SEM analysis reveal a thin surface layer at the anode side surface with low crystallinity caused by the depletion of Li during thermal poling. This work proved that with an open electrode setup similar results can be achieved as with a blocking setup.

The usage of a non-blocking setup with an open electrode configuration shows considerable advantages to a blocking setup with fully contacted electrodes. Although the setup shows some instability regarding electrical breakdowns for longer poling times, it offers new possibilities for further studies especially such as introducing different atmospheres, upscaling the treatment to larger samples and investigate a possible implementation of thermal poling into the ceramisation procedure. Specifically, the latter is interesting in industry applications. An open electrode configuration would allow modification of the glass and respective glass-ceramic in an inline and continuous, industrially applicable process.

Data availability statement

Data of presented results can be provided upon request.

Author contributions

Jonas Hildebrand: Conceptualization, Investigation, Data analysis, Visualization, Writing – original draft. Christian Roos: Conceptualization, Project administration, Resources, Funding acquisition, Writing – review and editing.

Competing interests

The authors declare that they have no competing interests.

Acknowledgement

The authors thank Schott AG for providing the used glass. We also thank Philipp Jacobs for performing the XRD measurements and Ralf Coenen for operating the SEM.

References

[1] D. E. Carlson, K. W. Hang, and G. F. Stockdale, 'Electrode "Polarization" in Alkali-Containing Glasses', J American Ceramic Society, vol. 55, no. 7, pp. 337–341, Jul. 1972, doi: 10.1111/j.1151-2916.1972.tb11305.x.

[2] M. Dussauze et al., 'How Does Thermal Poling Affect the Structure of Soda-Lime Glass?', J. Phys. Chem. C, vol. 114, no. 29, pp. 12754–12759, Jul. 2010, doi: 10.1021/jp1033905.

[3] A. Von Hippel, E. P. Gross, J. G. Jelatis, and M. Geller, 'Photocurrent, Space-Charge Buildup, and Field Emission in Alkali Halide Crystals', Phys. Rev., vol. 91, no. 3, pp. 568–579, Aug. 1953, doi: 10.1103/PhysRev.91.568.

[4] M. Chazot et al., 'Enhancement of mechanical properties and chemical durability of Soda-lime silicate glasses treated by DC gas discharges', J. Am. Ceram. Soc., vol. 104, no. 1, pp. 157–166, Jan. 2021, doi: 10.1111/jace.17438.

[5] J. Luo et al., 'Chemical structure and mechanical properties of soda lime silica glass surfaces treated by thermal poling in inert and reactive ambient gases', J Am Ceram Soc, vol. 101, no. 7, pp. 2951–2964, Jul. 2018, doi: 10.1111/jace.15476.

[6] H. An and S. Fleming, 'Second-order optical nonlinearity and accompanying near-surface structural modifications in thermally poled soda-lime silicate glasses', J. Opt. Soc. Am. B, vol. 23, no. 11, p. 2303, Nov. 2006, doi: 10.1364/JOSAB.23.002303.

[7] A. A. Lipovskii, A. I. Morozova, and D. K. Tagantsev, 'Giant Discharge Current in Thermally Poled Silicate Glasses', J. Phys. Chem. C, vol. 120, no. 40, pp. 23129–23135, Oct. 2016, doi: 10.1021/acs.jpcc.6b07144.

[8] A. V. Redkov, V. G. Melehin, and A. A. Lipovskii, 'How Does Thermal Poling Produce Interstitial Molecular Oxygen in Silicate Glasses?', J. Phys. Chem. C, vol. 119, no. 30, pp. 17298–17307, Jul. 2015, doi: 10.1021/acs.jpcc.5b04513.

[9] J. Luo, H. He, N. J. Podraza, L. Qian, C. G. Pantano, and S. H. Kim, 'Thermal Poling of Soda-Lime Silica Glass with Nonblocking Electrodes-Part 1: Effects of Sodium Ion Migration and Water Ingress on Glass Surface Structure', J. Am. Ceram. Soc., vol. 99, no. 4, pp. 1221–1230, Apr. 2016, doi: 10.1111/jace.14081.

[10] H. Ikeda et al., 'Generation of alkali-free and high-proton concentration layer in a soda lime glass using non-contact corona discharge', Journal of Applied Physics, vol. 114, no. 6, p. 063303, Aug. 2013, doi: 10.1063/1.4817760.

[11] A. Okada, K. Ishii, K. Mito, and K. Sasaki, 'Phase-matched second- harmonic gene ration in novel corona poled glass waveguides', Appl. Phys. Lett., vol. 60, no. 23, pp. 2853–2855, Jun. 1992, doi: 10.1063/1.106845.

[12] A. Okada, K. Ishii, K. Mito, and K. Sasaki, 'Second-order optical nonlinearity in corona-poled glass films', Journal of Applied Physics, vol. 74, no. 1, pp. 531–535, Jul. 1993, doi: 10.1063/1.355265.

[13] S. Horinouchi, H. Imai, G. J. Zhang, K. Mito, and K. Sasaki, 'Optical quadratic nonlinearity in multilayer corona-poled glass films', Appl. Phys. Lett., vol. 68, no. 25, pp. 3552–3554, Jun. 1996, doi: 10.1063/1.116634.

[14] S. Ettori, J.-C. Peraud, and J. Barton, 'Deionisation of glass by corona discharge', EP0237431B1 [Online]. Available: https://patents.google.com/patent/EP0237431B1/en

[15] M. Sander, P. Engelmann, P. Jacobs, and C. Roos, 'Controlled surface crystallization of lithium-zinc- alumosilicate glass- ceramics using thermal poling', J Am Ceram Soc, vol. 105, no. 5, pp. 3279–3290, May 2022, doi: 10.1111/jace.18301.

[15] M. Sander, 'Structure and properties of thermally poled lithium alumosilicate glasses and glass-ceramics', Ph.D. dissertation, Dept. of Glass and Glass-Ceramic, RWTH Aachen University, Aachen, Germany, 2023.

[17] N. Ikutame et al., ‘Low-temperature fabrication of fine structures on glass using electrical nanoimprint and chemical etching’, Journal of Applied Physics, vol. 114, no. 8, p. 083514, Aug. 2013, doi: 10.1063/1.4819321.
[18] W. Margulis and F. Laurell, ‘Interferometric study of poled glass under etching’, Opt. Lett., vol. 21, no. 21, p. 1786, Nov. 1996, doi: 10.1364/OL.21.001786.
[19] A. Lepicard et al., ‘Surface Reactivity Control of a Borosilicate Glass Using Thermal Poling’, J. Phys. Chem. C, vol. 119, no. 40, pp. 22999–23007, Oct. 2015, doi: 10.1021/acs.jpcc.5b07139.
[20] A. N. Kamenskii, I. V. Reduto, V. D. Petrikov, and A. A. Lipovskii, ‘Effective diffraction gratings via acidic etching of thermally poled glass’, Optical Materials, vol. 62, pp. 250–254, Dec. 2016, doi: 10.1016/j.optmat.2016.09.074.
[21] H. He, J. Luo, L. Qian, C. G. Pantano, and S. H. Kim, ‘Thermal Poling of Soda-Lime Silica Glass with Nonblocking Electrodes-Part 2: Effects on Mechanical and Mechanochemical Properties’, J. Am. Ceram. Soc., vol. 99, no. 4, pp. 1231–1238, Apr. 2016, doi: 10.1111/jace.14080.
[22] E. C. Ziemath, V. D. Araújo, and C. A. Escanhoela, ‘Compositional and structural changes at the anodic surface of thermally poled soda-lime float glass’, Journal of Applied Physics, vol. 104, no. 5, p. 054912, Sep. 2008, doi: 10.1063/1.2975996.
[23] M. Dussauze, E. I. Kamitsos, E. Fargin, and V. Rodriguez, ‘Refractive index distribution in the non-linear optical layer of thermally poled oxide glasses’, Chemical Physics Letters, vol. 470, no. 1–3, pp. 63–66, Feb. 2009, doi: 10.1016/j.cplett.2009.01.007.
[24] W. Margulis and F. Laurell, ‘Fabrication of waveguides in glasses by a poling procedure’, Applied Physics Letters, vol. 71, no. 17, pp. 2418–2420, Oct. 1997, doi: 10.1063/1.120079.
[25] A. Canagasabey, C. Corbari, Z. Zhang, P. G. Kazansky, and M. Ibsen, ‘Broadly tunable second-harmonic generation in periodically poled silica fibers’, Opt. Lett., vol. 32, no. 13, p. 1863, Jul. 2007, doi: 10.1364/OL.32.001863.
[26] P. St. J. Russell, C. N. Pannell, P. G. Kazansky, and L. Dong, ‘Pockels effect in thermally poled silica optical fibres’, Electronics Letters, vol. 31, no. 1, pp. 62–63, Jan. 1995, doi: 10.1049/el:19950036.
[27] B. H. O’Connor and M. D. Raven, ‘Application of the Rietveld Refinement Procedure in Assaying Powdered Mixtures’, Powder Diffr., vol. 3, no. 1, pp. 2–6, Mar. 1988, doi: 10.1017/S0885715600013026.